Highly Efficient Visible Light-Induced Ca^{2+} Chelation

Nishal M. Egodawaththa, Olivia Rajhel, Jingxuan Ma, Charitha Guruge, Alec B. Pabarue, Emily Harris, Roberto Peverati, Nasri Nesnas*

Department of Chemistry and Chemical Engineering, Florida Institute of Technology, Melbourne, Florida 32901, United States

Supporting Information Placeholder

Calcium ion (Ca^{2+}) control is an essential tool in neuronal research. Herein, we report three thiocoumarin-based, visible light-activated Ca^{2+} chelators with high quantum yields of 0.39, 0.52, and 0.83. The chelators demonstrated an over 10^5-fold increase in Ca^{2+} binding affinity upon irradiation. These chelators are efficiently triggered by biologically safer wavelengths, rendering them excellent candidates for use in neuroscientific research and medicine.

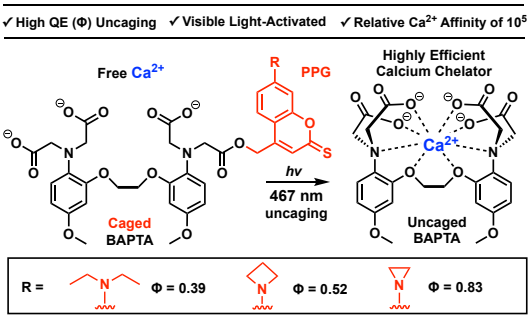

Calcium is an essential second messenger for communication across neurons.[1-4] Dysregulation of ionic calcium in the brain is a known cause of early cell death, and by extension, conditions such as Alzheimer's disease (AD), heart issues, and cancer.[5-7] Over the past 15 years, research on this correlation has rapidly gained momentum, rendering control over Ca^{2+} concentration a highly desirable tool.[8] However, while several photo-release systems for Ca^{2+} exist,[9-11] there are limited examples of molecules that can uptake Ca^{2+} upon irradiation. The only examples to date were reported by Roger Y. Tsien et al. in 1989 and 1997 with the design of two UV-responsive calcium ion uptake systems (Figure 1).[12,13] The first example involved the attachment of an *ortho*-nitrobenzyl (ONB) photolabile protecting group (PPG) to 1,2-bis(o-aminophenoxy)ethane-N,N,N',N'-tetraacetic acid (BAPTA).[12] The second replaced the ONB PPG with an azide for better efficiency.[13] In both systems, UV light irradiation leads to the detachment of the PPG, thereby releasing the calcium ion chelating moiety.[12-14] Since calcium ion modulation is critical in studying animal behavior, the design of efficient, visible light-triggered tools for calcium uptake is extremely valuable.[15-17]

The ONB- and azide-caged BAPTA moieties offer excellent foundations for photoactivatable Ca^{2+} chelators. However, their activation by UV light imposes severe limitations on potential neurobiological application due to the adverse effects of use in vivo. [18,19] These damaging effects are mainly resultant from the tendency of UV light to initiate undesirable photochemical side reactions[20,21] and generate toxic byproducts within the body.[20,22,23] Additionally, UV light has low penetration capabilities, further limiting application in deep tissues.[23,24]

In addition to being accompanied by the drawbacks of activation by UV light, these previously reported molecules suffer from low quantum yields, making them much less appealing for use.[25] Furthermore, they are limited in their fluorescence enhancement, rendering them less applicable in fluorescence-based probes.[26-29]

While current BAPTA-based molecules provide a solid basis for effective Ca^{2+} chelators, less phototoxic and more effective cages are needed.[12,30] Inspired by this need and the work of those before us, we hereby introduce three photolabile dimethoxy-BAPTA-based Ca^{2+} chelators photo-triggered in the visible light spectrum and with quantum yields as high as 0.83.

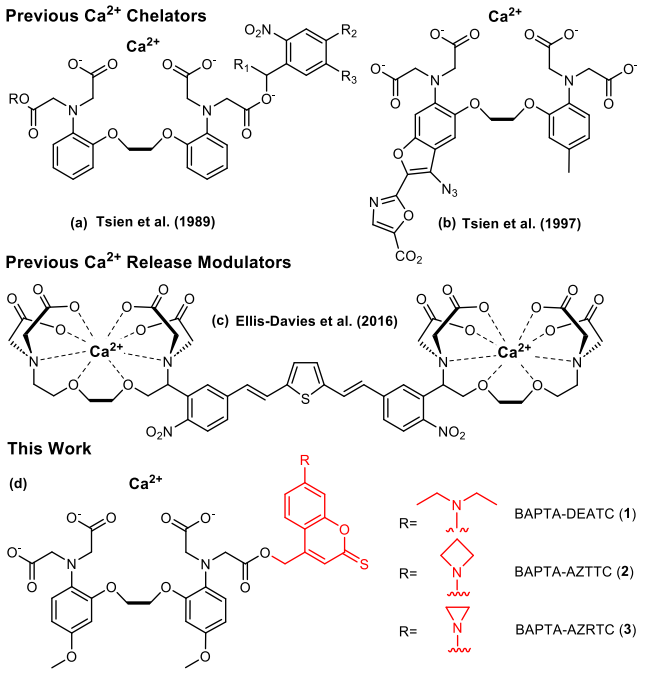

Figure 1. (a) UV-responsive ONB-caged Ca^{2+} chelator synthesized by Tsien, 1989, (b) UV-responsive azide-caged Ca^{2+} chelator with increased efficiency synthesized by Tsien, 1997, (c) visible light-activated Ca^{2+} release modulator synthesized by Ellis-Davies, 2016, and (d) the three visible light-activated Ca^{2+} chelators presented in this work.[9–13]

The caged Ca^{2+} chelators described herein are comprised of two parts: the thionyl coumarin PPG unit and the dimethoxy-BAPTA-based Ca^{2+} chelator. The syntheses of the

PPGs were accomplished by modifying the commercially available 7-diethylamino-4-methyl-coumarin (**6**), the synthesized 7-azetidin-1-yl-4-methyl-coumarin (**7**), and the synthesized 7-aziridin-1-yl-4-methyl-coumarin (**8**) (Scheme 1). The latter precursors, **7** and **8**, were prepared from 3-bromophenol (**4**) via a reaction with ethyl acetoacetate under strongly acidic conditions. This was followed by a Buchwald-Hartwig[31] coupling with the corresponding strained cyclic amine, azetidine, and aziridine, leading to **7** and **8** respectively. Subsequent modifications were accomplished via oxidization of the 4-methyl groups of each precursor to its corresponding aldehyde, **9**, **10**, and **11**, using selenium dioxide (SeO_2).[32] Then, the aldehydes were reduced to their corresponding alcohols, **12**, **13**, and **14**, using sodium borohydride ($NaBH_4$). Subsequently, the alcohols were protected with an acetate ester[33] to accommodate the thiolation of the lactone oxygen in the C-2 position. Lawesson's reagent was used for the thiolation to generate compounds **18**, **19**, and **20**.[33,34] Finally, the alcohol was deprotected to attain the desired thionyl coumarin PPGs, compounds **21**, **22**, and **23**, as shown in Scheme 1.[20,21,35-39]

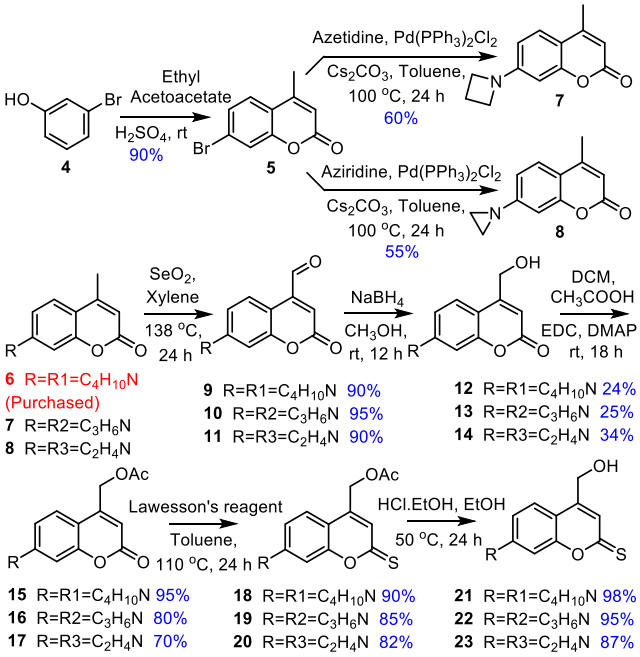

Scheme 1. Synthesis of the thionyl coumarin PPGs.

Our Ca^{2+} chelators took advantage of the electron donating capabilities of methoxy groups. By incorporating a para methoxy group into BAPTA, we achieved a remarkable 1.8-fold improvement compared to para unsubstituted aromatic rings.[40] Other reports demonstrated that withdrawing groups such as para-dibromo and para-dinitro have weaker chelating affinities toward Ca^{2+} than the unsubstituted BAPTA. The dimethoxy-BAPTA used in this work reflects a 29-fold and a 126×10^3-fold improvement in Ca^{2+} binding relative to the para-dibromo and dinitro-BAPTA respectively.[40,41] This underscores the remarkable efficacy of our modified chelators in modulating Ca^{2+} binding interactions.

Initially, we dimerized a 5-methoxy-2-nitrophenol (**24**) with a 1,2-dibromoethane (**25**) to yield compound **26**. Then, the two nitro groups in **26** were reduced to amines by hydrogen with Pd/C. Compound **27** was reacted with *tert*-butyl bromoacetate (**28**) in the presence of a proton sponge to afford **29**. We used *tert*-butyl bromoacetate due to the ease of selective deprotection of the tertiary butyl group. Mild conditions using trifluoroacetic acid (TFA) at 0˚C for only 1 h ensured partial deprotection such that only one of the four *tert*-butyl groups in **29** was removed. The synthesis of the modified BAPTA is illustrated in Scheme 2.

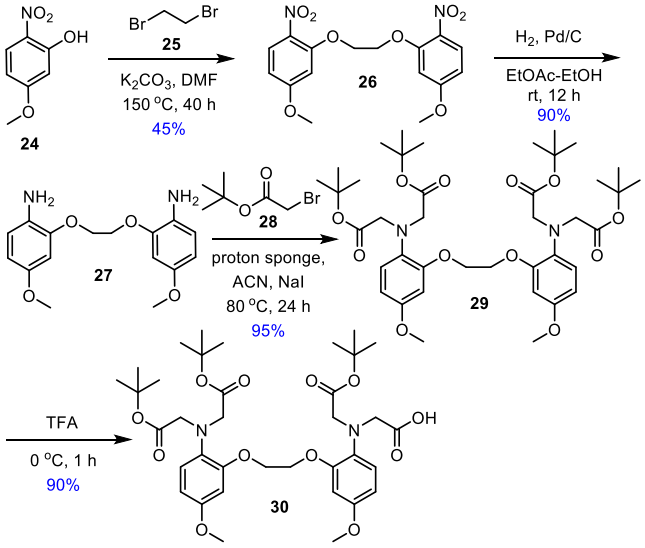

Scheme 2. Synthesis of the dimethoxy-BAPTA moiety.

The synthesized thionyl coumarin PPG precursors, **21**, **22**, and **23**, and compound **30**, were esterified using EDC coupling with DMAP to form the three caged dimethoxy-BAPTA molecules. The obtained products, **31**, **32**, and **33**, were purified by column chromatography. Then, the remaining *tert*-butyl groups were exhaustively deprotected using TFA to afford target products **1**, **2**, and **3** as depicted in Scheme 3.

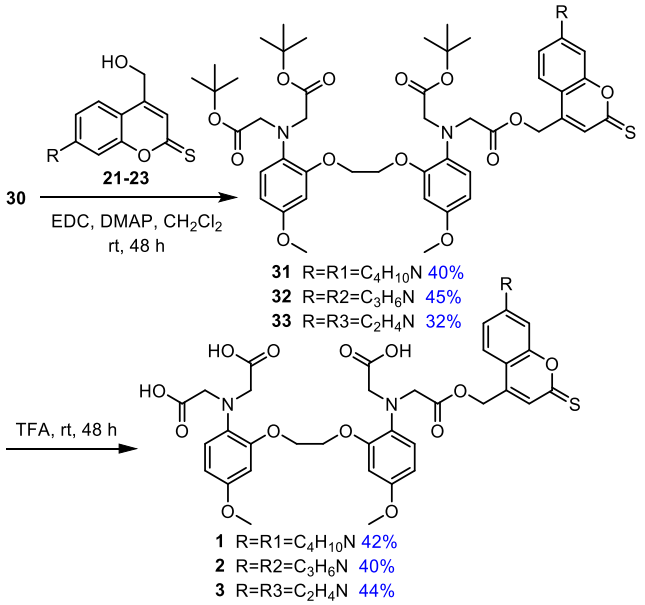

Scheme 3. Reaction of thionyl coumarin with dimethoxy-BAPTA.

Herein, from this synthesis, we report three novel caged calcium chelators that uptake Ca^{2+} upon irradiation by blue light at 467 nm. A comparison of the quantum yields of these caged systems is illustrated in Scheme 4.

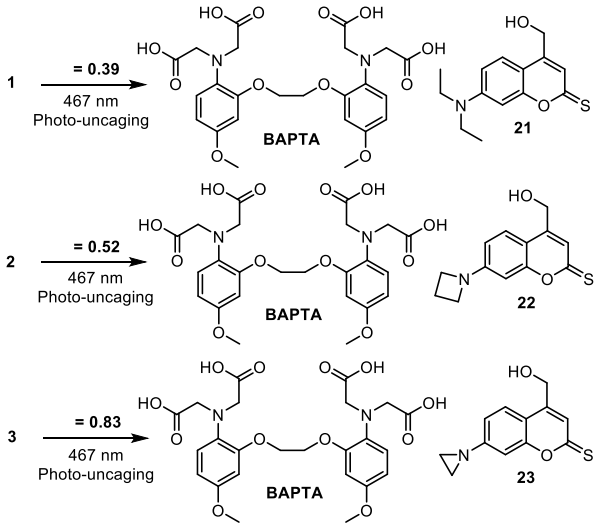

Scheme 4. Photo-uncaging and quantum yield comparison of 7-Diethylamino-4-thiocoumarin-BAPTA (**1**), 7-Azetidin-4-thiocoumarin-BAPTA (**2**), and 7-Aziridin-4-thiocoumarin-BAPTA (**3**).

Visible light-responsive systems are critical for biological research.[26,42-44] The light responsiveness for compounds **1**-**3** was evaluated by measuring the quantum yields (ϕ) of uncaging. We employed sequential NMR analysis to quantify the depletion of the starting material with irradiation time.[44,48,49] The concentration depletion of the compounds obeys the pseudo-first-order rate law, as displayed in Figure 2. As a result, all three caged molecules could be employed for use in neuroscience with relatively high concentrations.

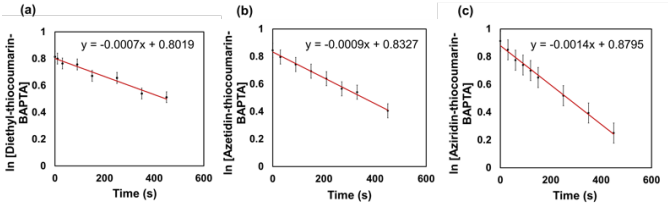

Figure 2. Rate of photolysis for (a) **1**, (b) **2**, and (c) **3**.

The following equation was used to calculate the quantum yield of each caged molecule.[44,48-50]

$$\phi = \frac{-d[cage]}{dt} \times \frac{VN_AE_\lambda}{FA(1-10^{-\varepsilon b[C]})}$$

The dataset includes key parameters such as the maximum absorbance wavelength (λ_{max}), molar extinction coefficient (ε), power density of the light source or light flux (F, Wm^{-2}), volume (V, L), Avogadro's number (N_A, mol^{-1}), energy (E_λ, $J.photon^{-1}$), area (A, m^2), path length (b, cm), and concentration of the caged molecule (C, $molL^{-1}$). Quantum yields (ϕ), and photocrossed sections ($\varepsilon\phi$) were computed and are presented in Table 1. We determined the light flux using liquid-phase potassium ferrioxalate actinometry.[44] **3** exhibited the highest quantum yield (0.83), attributable to the heightened ring and torsional strain inherent in the three-membered aziridine ring.[51-54] Ring strain arises when the bond angles in a cyclic structure deviate from the ideal angles, leading to increased energy.[52,54] Higher ring strain can result in more energetic intermediates during photochemical processes, potentially contributing to a higher quantum yield.[54] In contrast, the four-membered azetidine ring in **2** experiences lower ring strain, likely accounting for its comparatively lower quantum yield.

Table 1. Photochemical properties of **1**, **2**, and **3**.

Cage	λ_{Max}/nm	$\varepsilon(\lambda_{Max})/M^{-1}cm^{-1}$	Φ	$\varepsilon\phi/M^{-1}cm^{-1}$
1	469	23009	0.39±0.01	8.9×10^3
2	473	20542	0.52±0.02	1.1×10^3
3	475	15664	0.83±0.01	1.3×10^3

The surface plasmon resonance (SPR) band (460-500 nm) of caged compounds **1**, **2**, and **3** exhibited a decrease during 50 s of total irradiation. This shift in the SPR band suggests a photoinduced alteration in the electronic structure of the caged compounds during the irradiation process. The corresponding UV spectra for the caged molecules can be found in the Supporting Information. The calcium affinity of the dimethoxy-BAPTA and caged compounds were determined by spectrophotometric titration at a pH of 7.4 using HEPES buffer solution.[55-57] The absorbance of dimethoxy-BAPTA steadily decreased with successive additions of $CaCl_2$ until it leveled off above 2.5 μM Ca^{2+}, while **1**, **2**, and **3** failed to reach above 0.5 μM of Ca^{2+} (Figure 3d). We conducted comparisons of titrimetrically obtained binding constant values for the three caged molecules against the independent dimethoxy-BAPTA moiety. Dimethoxy-BAPTA alone demonstrated highly efficient chelation with a binding affinity of $1.8 \bullet 10^7$ M^{-1}. The high affinity of BAPTA to Ca^{2+} results from the negatively charged carboxylate groups on the octa-dentate ligand. However, **1**, **2**, and **3** had binding efficiencies of 36.6 M^{-1}, 32.2 M^{-1}, and 25.4 M^{-1} respectively, with an average value over 5.8 x 10^5 times lower than the value found for dimethoxy-BAPTA. The decrease in affinity confirms that the PPG effectively disrupts chelation as it occupies one of the carboxylate groups on the dimethoxy-BAPTA. This suggests a lower binding affinity of the caged molecules compared to dimethoxy-BAPTA.

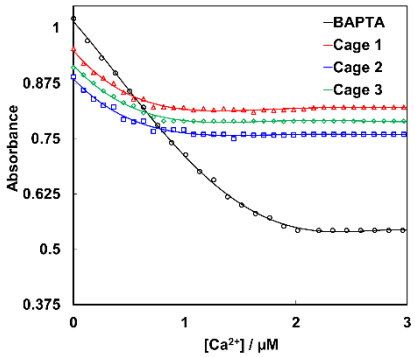

Figure 3. Data for the spectrophotometric titration of 47.6 μM aqueous solution of **1**,**2**, and **3** with 0.225 μM of $CaCl_2$ to determine Ca^{2+} binding affinity.

A preliminary computational investigation of the affinity of each of the cages to Ca^{2+} was conducted using density functional theory calculations. All calculations were performed in gas phase using the PBEh-3c composite method as implemented in the Q-Chem software.[58,59] The binding energies between Ca^{2+} and each cage, as well as dimethoxy-BAPTA, were calculated using optimized geometries of the

complexes and the unbound molecules. Results show that the three cages have binding energies to Ca^{2+} that are very similar to each other: **1**: –669. kcal/mol, **2**: –669. kcal/mol, and **3**: –673. kcal/mol. Dimethoxy-BAPTA alone, however, has a calculated binding energy to Ca^{2+} of –815. kcal/mol, which is at least 142 kcal/mol stronger than for each of the three cages (Figure 4). These results align with the experimental binding efficiencies reported above and help explain the observed 10^5 times difference in Ca^{2+} affinity between the caged molecules and dimethoxy-BAPTA. The structural analysis reveals that the complex formed by dimethoxy-BAPTA is octa-dentate, with four atoms in the first shell of vdW radii at 2.30±0.05 Å from the central Ca^{2+} and four other atoms in the second shell at 3.00±0.05 Å. The complexes formed by **1**, **2**, and **3** are effectively hepta-coordinated, with three oxygen atoms at 2.23±0.03 Å and the three remaining oxygen atoms at distances ranging from 2.37 to 3.05 Å, one nitrogen atom at 2.70±0.05 Å, and the second nitrogen atom at 3.37±0.20 Å, a distance that is outside the second complexation shell. The computational results for the binding distances and partial charges of all molecules are reported in the Supporting Information.

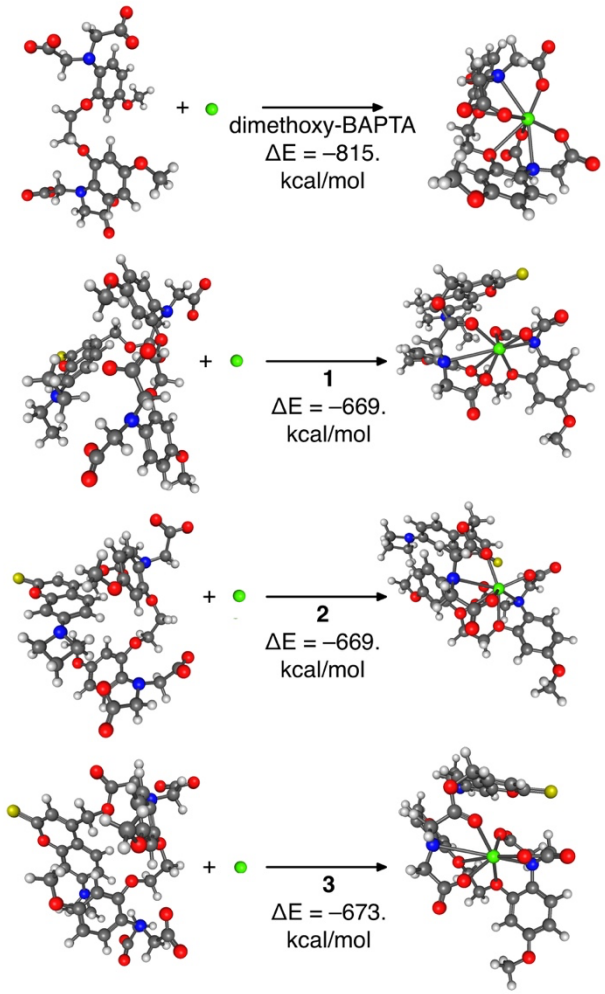

Figure 4. Binding energies of the caged molecules compared to dimethoxy-BAPTA using the PBEh-3c composite method.

We also noted that the three thiocoumarin scaffolds exhibited high fluorescence activity, enabling broader application. Due to their fluorescence capabilities, these caged molecules are viable for use as fluorophores in future biochemical investigation.[27,60-62] For example, fluorophores integrating these thiocoumarin scaffolds can be used for observing the dynamics of enzymes and their interactions within the biosystem via real-time fluorescence imaging.[28,29,63] Laser scanning confocal microscopy was used for high-resolution fluorescence imaging of all three cages on exact planes, allowing for better overall object visualization. We analyzed the 3D planes and depth of the caged molecules by stacking several images from different optical levels. The data from this analysis is included in the Supporting Information. Four different wavelengths were utilized in the emission parameters, allowing for the observation of fluorescence active sites with varying emission colors. The caged dimethoxy-BAPTA complex exhibits high fluorescence activity, yet the thiocoumarin PPG alone only demonstrates a fraction of the same fluorescence output. In the biological analysis of these chelators, this difference can be exploited for tracking the caged or uncaged state of the dimethoxy-BAPTA moiety.

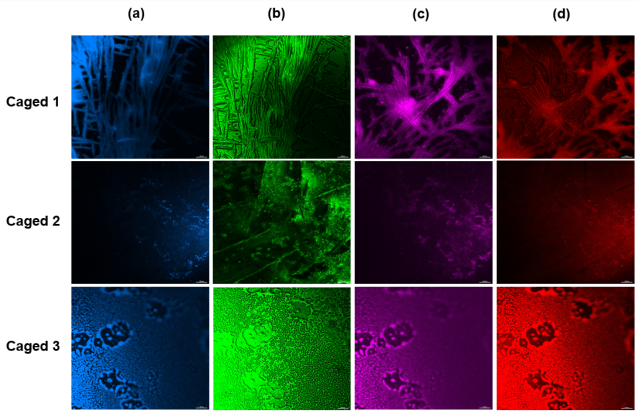

Figure 5. Images of **1**, **2**, and **3** with 4-Line Solid State Laser Confocal System with Nikon Eclipse Ti2 Inverted Microscope. The sample was excited with the laser at (a) 405 nm, (b) 488 nm, (c) 561 nm, and (d) 640 nm wavelengths, and the emission was observed at 424–483 nm, 502–522 nm, 552–581 nm, and 655-688 nm respectively.

In summary, we developed three blue-light-activated Ca^{2+} chelators with quantum yields of 0.39, 0.52, and 0.83. These molecules are the first Ca^{2+} chelators in literature to be activated by visible light. The 7-aziridin-4-thiocoumarin-BAPTA, **3**, had the highest reported quantum efficiency of the three synthesized chelators. Furthermore, binding affinity of the blue light-released dimethoxy-BAPTA was nearly a million times greater than that of the caged molecules. These three new caged Ca^{2+} chelators represent safer and more efficient options with strong potential for future use in neuroscientific research and medicine.[45-48] We are currently collaborating with neuroscientists who are testing the biological functionality of these photoreleasable Ca^{2+} chelators.

ASSOCIATED CONTENT

Supporting Information

The Supporting Information is available free of charge on the ACS Publications website.

Data Availability Statement

The data underlying this study is available in the published article and its Supporting Information.

AUTHOR INFORMATION

Corresponding Author

Nasri Nesnas –Department of Chemistry and Chemical Engineering, Florida Institute of Technology
email: nesnas@fit.edu

Authors

Roberto Peverati –Department of Chemistry and Chemical Engineering, Florida Institute of Technology
email: rpeverati@fit.edu
Nishal M. Egodawaththa –Department of Chemistry and Chemical Engineering, Florida Institute of Technology
email: enishalmaduj2020@my.fit.edu
Jingxuan Ma –Department of Chemistry and Chemical Engineering, Florida Institute of Technology
email: jma2014@my.fit.edu
Charitha Guruge –Department of Chemistry and Chemical Engineering, Florida Institute of Technology
email: cguruge2014@my.fit.edu
Olivia Rajhel –Department of Chemistry and Chemical Engineering, Florida Institute of Technology
email: orajhel2021@my.fit.edu
Alec B. Pabarue– Department of Chemistry and Chemical Engineering, Florida Institute of Technology
email: *apabarue3@gatech.edu*
Emily Harris –Department of Chemistry and Chemical Engineering, Florida Institute of Technology
email: eharris2020@my.fit.edu

Author Contributions

N.N. supervised the design, synthesis, and evaluation of molecules and R.P. supervised all computations. N.N., N.M.E., C.G., and O.R. designed the experiments. N.M.E, J.M, C.G., A.B.P., and E.H. performed the synthesis of the caged chelators. N.M.E., J.M., C.G., O.R., A.B.P., and E.H. characterized the synthesized compounds. N.M.E. and O.R. performed fluorescence microscopy studies. R.P. performed the computational analysis. The manuscript was written by N.N., N.M.E., and O.R. with contributions from all authors.

Notes
The authors declare no competing financial interest.

ACKNOWLEDGMENT

The authors would like to thank Alexzandriea van Hoekelen, Antonella Ambrosini, Nikola Mekic, and Sarah Yaseen for useful discussions and roles in the editing of the manuscript. This work was fully supported by NIH Grant (2R15-GM112119-02). Fluorescence imaging was carried out at the High-Resolution Microscopy and Advanced Imaging Center of the Florida Institute of Technology under the supervision of Dr. Tatiana Karpova. HRMS spectroscopy was conducted at the Mass Spectrometry Research and Education Center, University of Florida, with funding from NIH S10 OD021758-01A1. This article is dedicated in memory of the late Professors Koji Nakanishi and Ronald Breslow (Columbia University).

REFERENCES

(1) Bollimuntha, S.; Pani, B.; Singh, B. B. Neurological and Motor Disorders: Neuronal Store-Operated Ca^{2+} Signaling: An Overview and Its Function. *Adv. Exp. Med. Biol.* **2017**, *993*, 535–556.
(2) Kuran, M.; Tuğcu, T.; Edis, B. Ö. Calcium Signaling: Overview and Research Directions of a Molecular Communication Paradigm. *IEEE Wirel. Commun.* **2012**, *19*, 20–27.
(3) Soliven, B. Calcium Signalling in Cells of Oligodendroglial Lineage. *Microsc. Res. Techniq.* **2001**, *52*, 672–679.
(4) Nowycky, M.C.; Thomas, A. P. Intracellular Calcium Signaling. *J. Cell. Sci.* **2002**, *115*, 3715–3716.
(5) Jin, Z.; El-Deiry, W. S. Overview of Cell Death Signaling Pathways. *Cancer Biol. Ther.* **2005**, *4*, 147–171.
(6) Mattson, M. P.; Arumugam, T. V. Hallmarks of Brain Aging: Adaptive and Pathological Modification by Metabolic States. *Cell Metab.* **2018**, *27*, 1176–1199.
(7) Mayer, E. A. Neuronal Communication. *Neurosignals* **1993**, *2*, 57–76.
(8) Clapham, D. E. Calcium Signaling. *Cell* **2007**, *14*, 1047–1058.
(9) Ellis-davies, G. C. R.; Kaplan, J. H. Nitrophenyl-EGTA, A Photolabile Chelator That Selectively Binds Ca^{2+} with High Affinity and Releases it Rapidly upon Photolysis. *Proc. Natl. Acad. Sci.* **1994**, *91*, 187–191.
(10) Agarwal, H. K.; Janicek, R.; Chi, S.; Perry, J. W.; Niggli, E.; Ellis-davies, G. C. R. Calcium Uncaging with Visible Light. *J. Am. Chem. Soc.* **2016**, *138*, 3687–3693.
(11) Heckman, L. M.; Grimm, J. B.; Schreiter, E. R.; Kim, C.; Verdecia, M. A.; Shields, B. C.; Lavis, L. D. Design and Synthesis of a Calcium-Sensitive Photocage. *Angew. Chem. Int. Ed.* **2016**, *55*, 8363–8366.
(12) Adams, S. R.; Kao, J. P. Y.; Tsien, R. Y. Biologically Useful Chelators That Take Up Calcium (2+) Upon Illumination. *J. Am. Chem. Soc.* **1989**, *20*, 7957–7968.
(13) Adams, R.; Lev-ram, V.; Tsienl, R. Y. A New Caged Ca^{2+}, Azid-1, Is Far More Photosensitive than Nitrobenzyl-Based Chelators. *Chem. Biol.* **1997**, *4*, 867–878.
(14) Tsien, R. Y. New Calcium Indicators and Buffers with High Selectivity Against Magnesium and Protons: Design, Synthesis, and Properties of Prototype Structures. *Biochem.* **1980**, *19*, 2396–2404.
(15) Ghosh, A.; Greenberg, M. E. Calcium Signaling in Neurons: Molecular Mechanisms and Cellular Consequences. *Science* **1995**, *268*, 239–247.
(16) Bootman, M. D.; Bultynck, G. Fundamentals of Cellular Calcium Signaling: A Primer. *Cold Spring Harb. Perspect. Bio.* **2019**, *12*, 038802.
(17) Qian, Y.; Cosio, D. M.; Piatkevich, K. D.; Aufmkolk, S.; Su, W. C.; Celiker, O. T.; Schohl, A.; Murdock, M. H.; Aggarwal, A.; Chang, Y.; Wiseman, P. W.; Ruthazer, E. S.; Boyden, E. S.; Campbell, R. E. Improved Genetically Encoded Near-Infrared Fluorescent Calcium Ion Indicators for in Vivo Imaging. *PLOS Bio.* **2020**, *18*, 3000965.
(18) Burgalossi, A.; Jung, S; Man, K. N. M.; Nair, R.; Jockusch, W. J.; Wojcik, S. M.; Brose, N.; Rhee, J. Analysis of Neurotransmitter Release Mechanisms by Photolysis of Caged Ca^{2+} in an Autaptic Neuron Culture System. *Nat. Protoc.* 2012, *7*, 1351-1365.
(19) Ai, X.; Mu, J.; Xing, B. Recent Advances of Light-Mediated Theranostics. *Theranostics* **2016**, *6*, 2439–2457.
(20) Lin, Q.; Yang, L.; Wang, Z.; Hua, Y.; Zhang, D.; Bao, B.; Bao, C.; Gong, X.; Zhu, L. Coumarin Photocaging Groups Modified with an Electron-Rich Styryl Moiety at the 3-Position: Long-Wavelength Excitation, Rapid. Angew. *Chem. Int. Ed.* **2018**, *57*, 3722–3726.
(21) Gandioso, A.; Contreras, S.; Melnyk, I.; Oliva, J.; Nonell, S.; Velasco, D. Development of Green/Red-Absorbing Chromophores Based on a Coumarin Scaffold That Are Useful as Caging Groups. *J. Org. Chem.* **2017**, *82*, 5398–5408.

(22) Šolomek, T.; Wirz, J.; Klán, P. Searching for Improved Photoreleasing Abilities of Organic Molecules. *Acc. Chem. Res.* **2015**, *48*, 3064–3072.
(23) Klán, P.; Šolomek, T.; Bochet, C. G.; Blanc, A.; Givens, R. S.; Rubina, M.; Popik, V. V.; Kostikov, A.; Wirz, J. Photoremovable Protecting Groups in Chemistry and Biology: Reaction Mechanisms and Efficacy. *Chem. Rev.* **2012**, *113*, 119–191.
(24) Weinstain, R.; Slanina, T.; Kand, D.; Klán, P. Visible-to-NIR-Light Activated Release: From Small Molecules to Nanomaterials. *Chem. Rev.* **2020**, *120*, 13135–13272.
(25) Ai, X.; Hu, M.; Xing, B. Photoactivatable Targeting Methods. *Handbook of In Vivo Chemistry in Mice* **2019**, *14*, 401-432.
(26) Gandioso, A.; Nin-hill, A.; Melnyk, I.; Rovira, C. Sequential Uncaging with Green Light Can Be Achieved by Fine-Tuning the Structure of a Dicyanocoumarin Chromophore. *ChemistryOpen* **2017**, *6*, 375–384.
(27) Cho, M.; Nguyen, V.; Yoon, J. Simultaneous Detection of Hypochlorite and Singlet Oxygen by a Thiocoumarin-Based Ratiometric Fluorescent Probe. *ACS Measurement Au* **2022**, *2*, 219–223.
(28) Hirabayashi, K.; Hanaoka, K.; Egawa, T.; Kobayashi, C. Cell Calcium Development of Practical Red Fluorescent Probe for Cytoplasmic Calcium Ions with Greatly Improved Cell-Membrane Permeability. *Cell Calcium* **2016**, *60*, 256–265.
(29) Egawa, T.; Hirabayashi, K.; Koide, Y.; Kobayashi, C.; Takahashi, N.; Mineno, T.; Terai, T.; Ueno, T.; Komatsu, T.; Ikegaya, Y.; Matsuki, N.; Nagano, T.; Hanaoka, K. Red Fluorescent Probe for Monitoring the Dynamics of Cytoplasmic Calcium Ions. *Angew. Chem. Int. Ed.* **2013**, *52*, 3874–3877.
(30) Tymianski, M.; Charlton, M. P.; Carlen, P. L.; Tator, C. H. Properties of Neuroprotective Cell-permeant Ca^{2+} Chelators: Effects on $[Ca^{2+}]_i$ and Glutamate Neurotoxicity in Vitro. *J. Neurophysiol*. **1994**, *72*, 1973-1992.
(31) Lim, T.; Byun, S.; Kim, B. M. Pd(PPh_3)$_4$-Catalyzed Buchwald–Hartwig Amination of Aryl Fluorosulfonates with Aryl Amines. *Asian J. Org. Chem*. **2017**, *6*, 1222-1225.
(32) Toan, V. N.; Thành, N. Đ. Synthesis of 6- and 7-Alkoxy-4-Methylcoumarins from Corresponding Hydroxy Coumarins and Their Conversion into 6- and 7-Alkoxy-4-Formylcoumarin Derivatives. *Synth. Commun.* **2020**, *50*, 3603–3615.
(33) Fournier, L.; Gauron, C.; Xu, L.; Aujard, I.; Saux, T. Le; Gagey-eilstein, N.; Maurin, S.; Dubruille, S.; Baudin, J.; Bensimon, D.; Volovitch, M.; Vriz, S.; Jullien, L. Blue-Absorbing Photolabile Protecting Group for in vivo Chromatically Orthogonal Photoactivation. *ACS Chem. Biol.* **2013**, *8*, 1528–1536.
(34) Fournier, L.; Aujard, I.; Saux, L.; Maurin, S. Coumarinylmethyl Caging Groups with Redshifted Absorption. *Chem. Eur. J.* **2013**, *19*, 17494–17507.
(35) Olson, J. P.; Kwon, H.; Takasaki, K. T.; Chiu, C. Q.; Higley, M. J.; Sabatini, B. L.; Ellis-davies, G. C. R. Optically Selective Two-Photon Uncaging of Glutamate at 900 nm. *J. Am. Chem. Soc.* **2013**, *135*, 5954–5957.
(36) Furuta, T.; Takeuchi, H.; Isozaki, M.; Takahashi, Y.; Kanehara, M.; Sugimoto, M.; Watanabe, T.; Noguchi, K.; Dore, T. M.; Kurahashi, T.; Iwamura, M.; Tsien, R. Y. Bhc-CNMPs as Either Water-Soluble or Membrane-Permeant Photoreleasable Cyclic Nucleotides for Both One- and Two-Photon Excitation. *ChemBioChem* **2004**, *5*, 1119–1128.
(37) Bao, C.; Fan, G.; Lin, Q.; Li, B.; Cheng, S.; Huang, Q. Styryl Conjugated Coumarin Caged Alcohol: Efficient Photorelease by Either One-Photon Long Wavelength or Two-Photon NIR Excitation. *Org. Lett.* **2011**, *14*, 3729–3732.
(38) Bassolino, G.; Nançoz, C.; Thiel, Z.; Bois, E.; Vauthey, E.; Rivera-Fuentes, P. Photolabile Coumarins with Improved Efficiency through Azetidinyl Substitution. *Chem. Sci.* **2018**, *9*, 387–391.
(39) Ma, J.; Ripp, A.; Wassy, D.; Dürr, T.; Qiu, D.; Häner, M.; Haas, T.; Popp, C.; Bezold, D.; Richert, S.; Esser, B.; Jessen, H. J. Thiocoumarin Caged Nucleotides: Synthetic Access and Their Photophysical Properties. *Molecules* **2020**, *25*, 5325.
(40) Adler, E. M.; Augustine, G. J.; Duffy, S.; Charlton, M. P. Alien Intracellular Calcium Chelators Attenuate Neurotransmitter Release at the Squid Giant Synapse. *J. Neurosci.* **1991**, 11, 1496–1507.
(41) Ducrot, A.; Tron, A.; Bofinger, R.; Beguer, I. S.; Pozzo, J.; McClenaghan, N. D. Photoreversible Stretching of a BAPTA Chelator Marshalling Ca^{2+}-Binding in Aqueous Media. *Beilstein J. Org. Chem.* 2019, 15, 2801–2811.
(42) Hagen, V.; Dekowski, B.; Nache, V.; Schmidt, R.; Geißler, D.; Lorenz, D.; Eichhorst, J.; Keller, S.; Kaneko, Hiroshi. Benndorf, Klaus.; Wiesner, B. Coumarinylmethyl Esters for Ultrafast Release of High Concentrations of Cyclic Nucleotides upon One- and Two-Photon Photolysis. *Angew. Chem. Int. Ed.* **2005**, *44*, 7887–7891.
(43) Hansen, M. J.; Velema, W. A.; Lerch, M. M.; Szymanski, W.; Feringa, B. L. Wavelength-Selective Cleavage of Photoprotecting Groups: Strategies and Applications in Dynamic Systems. *Chem. Soc. Rev.* **2015**, *44*, 3358–3377.
(44) Ma, J.; Egodawaththa, N. M.; Guruge, C.; Márquez, O. A. V.; Likes, M.; Nesnas, N. Blue and Green Light Responsive Caged Glutamate. *J. Photochem. Photobio. A. Chem.* **2024**, *447*, 115183.
(45) Guruge, C.; Ouedraogo, Y. P.; Comitz, R. L.; Ma, J.; Losonczy, A.; Nesnas, N. Improved Synthesis of Caged Glutamate and Caging Each Functional Group. *ACS Chem. Neurosci.* **2018**, *9*, 2713–2721.
(46) Comitz, R. L.; Ouedraogo, Y. P.; Nesnas, N. Unambiguous Evaluation of the Relative Photolysis Rates of Nitro Indolinyl Protecting Groups Critical for Brain Network Studies. *Anal. Chem. Res.* **2015**, *3*, 20–25.
(47) Ellis-Davies, G. C. R. Caged Compounds: Photorelease Technology for Control of Cellular Chemistry and Physiology. *Nat. Methods.* **2007**, *4*, 619–628.
(48) Padwa, A. Azirine Photochemistry. *Acc. Chem. Res.* **1976**, *9*, 371–378.
(49) Dequina, H. J.; Jones, C. J.; Schomaker, J. M. Recent Updates and Future Perspectives in Aziridine Synthesis and Reactivity. *Chem.* **2023**, *9*, 1658–1701.
(50) Lopes, S.; Reva, I.; Fausto, R. Infrared Spectra and UV-Induced Photochemistry of Methyl Aziridine-2-carboxylate Isolated in Argon and Xenon Matrices. *Vib. Spectrosc.* **2015**, *81*, 68–82.
(51) Liu, X.; Qiao, Q.; Tian, W.; Liu, W.; Chen, J.; Lang, M. J.; Xu, Z. Aziridinyl Fluorophores Demonstrate Bright Fluorescence and Superior Photostability by Effectively Inhibiting Twisted Intramolecular Charge Transfer. *J. Am. Chem. Soc.* **2016**, *138*, 6960–6963.
(52) Cui, J.; Gropeanu, R. A.; Stevens, D. R.; Rettig, J.; Del Campo, A. New Photolabile BAPTA-Based Ca^{2+} Cages with Improved Photorelease. *J. Am. Chem. Soc.* **2012**, *134*, 7733–7740.
(53) Pethig, R.; Kuhn, M.; Payne, R.; Adler, E. M.; Chen, T.; Jaffe, L. F. On the Dissociation Constants of BAPTA-type Calcium Buffers. *Cell Calcium* **1989**, *10*, 491–498.
(54) Sutton, M. V.; McKinley, M.; Kulasekharan, R.; Popik, V. V. Photo-cleavable Analog of BAPTA for the Fast and Efficient Release of Ca^{2+}. *ChemComm*. **2017**, *53*, 5598–5601.
(55) Grimme, S.; Brandenburg, J. G.; Bannwarth, C.; Hansen, A. Consistent Structures, and Interactions by Density

Functional Theory with Small Atomic Orbital Basis Sets. *J. Chem. Phys.* **2015**, *143*, 054107.
(56) Epifanovsky, E.; Gilbert, A. T. B.; Feng, X.; Lee, J.; Mao, Y.; Mardirossian, N.; Pokhilko, P.; White, A. F.; Coons, M. P.; Dempwolff, A. L.; et al. Software for the Frontiers of Quantum Chemistry: An Overview of Developments in the Q-Chem 5 Package. *J. Chem. Phys.* **2021**, *155*, 084801.
(57) Zhao, Y.; Zheng, Q.; Dakin, K.; Xu, K.; MartíNez, M.; Li, W. H. New Caged Coumarin Fluorophores with Extraordinary Uncaging Cross Sections Suitable for Biological Imaging Applications. *J. Am. Chem. Soc.* **2004**, *126*, 4653–4663.
(58) Collot, M.; Loukou, C.; Yakovlev, A. V.; Wilms, C. D.; Li, D.; Evrard, A.; Zamaleeva, A.; Bourdieu, L.; Léger, J. F.; Ropert, N.; Eilers, J.; Oheim, M.; Feltz, A.; Mallet, J. M. Calcium Rubies: A Family of Red-Emitting Functionalizable Indicators Suitable for Two-Photon Ca^{2+} Imaging. *J. Am. Chem. Soc.* **2012**, *134*, 14923–14931.
(59) Gandioso, A.; Palau, M.; Bresolí-Obach, R.; Galindo, A.; Rovira, A.; Bosch, M.; Nonell, S.; Marchán, V. High Photostability in Nonconventional Coumarins with Far-Red/NIR Emission through Azetidinyl Substitution. *J. Org. Chem.* **2018**, *83*, 11519–11531
(60) Wu, X.; Li, H.; Lee, E.; Yoon, J. Sensors for *In Situ* Real-Time Fluorescence Imaging of Enzymes. *Chem* **2020**, *6*, 2893–2901.
(61) Gandioso, A.; Cano, M.; Massaguer, A. A Green Light-Triggerable RGD Peptide for Photocontrolled Targeted Drug Delivery: Synthesis and Photolysis Studies. *J. Org. Chem.* **2016**, *81*, 11556–11564.
(62) Schönleber, R. O.; Bendig, J.; Hagen, V.; Giese, B. Rapid Photolytic Release of Cytidine 5′-Diphosphate from a Coumarin Derivative: A New Tool for the Investigation of Ribonucleotide Reductases. *Bioorg. Med. Chem.* **2002**, *10*, 97–101.
(63) Guruge, C.; Rfaish, S. Y.; Byrd, C.; Yang, S.; Starrett, A. K.; Guisbert, E.; Nesnas, N. Caged Proline in Photoinitiated Organocatalysis. *J. Org. Chem.* **2019**, *84*, 5236–5244.